# External standard calibration method for high-repetition-rate shock tube kinetic studies with synchrotron-based time-of-flight mass spectrometry

F. E. Cano Ardila[1], S. Nagaraju[1], R. S. Tranter[2], S. Abid[1], A. Desclaux[1], A. Roque Ccacya[1], G. A. Garcia[3], N. Chaumeix[1], A. Comandini[1]
[1]Institut de Combustion, Aérothermique, Réactivité et Environnement, CNRS-INSIS, Orléans, France
[2]Chemical Sciences and Engineering Department, Argonne National Laboratory, Illinois USA
[3]Synchrotron SOLEIL, L'Orme des Merisiers, St. Aubin BP 48, 91192 Gif sur Yvette, France

## 1 Introduction

Among the different techniques in chemical kinetics, shock tubes are very versatile reactors which have been used in a large number of applications and experimental conditions. In particular, several laboratory-based diagnostics were coupled to shock tubes with the aim of measuring reaction intermediates and products, including single-pulse operation with gas sampling and analyses by gas chromatography and mass spectrometry (GC-MS) [1-3], time-of-flight mass spectrometry (TOF-MS) [4-5], and in-situ laser absorption measurements [6]. Since the development of the ANL miniature high repetition-rate shock tube (ANL-HRRST) by Tranter and Lynch [7], access to synchrotron-based diagnostics has also been possible. In particular, the ANL-HRRST has been primarily used at the Advanced Light Source (ALS) with TOF-MS (ANL-HRRST/TOF-MS) [8], while the HRRST built at ICARE (ICARE-HRRST) with double imaging photolelectron/photoion spectroscopy (i$^2$PEPICO) [9] at the DESIRS beamline of synchrotron SOLEIL [10]. While both apparatuses have produced considerable insight into complex reaction mechanisms it has so far not been possible to extract kinetic data from them. This is mainly because of the fast changes in pressure that occur within a shock tube experiment that induce a slower increase in pressure in the ion source of the spectrometer. This problem has been already addressed in conventional laboratory-based shock tube/TOF-MS kinetic investigations [4] with the use of an internal standard (e.g. argon). On the other hand, implementing an internal calibration method with PI sources is difficult primarily due to the lack of inert species that have ionization energies in the range of most organic molecules. In this work, we present an alternative method for calibrating the pressure response which we refer to as an external calibration. The method is tested on HRRST/ i$^2$PEPICO experiments on the pyrolysis of toluene.

**Correspondence to: andrea.comandini@cnrs-orleans.**

## 2 Experimental methods

The ICARE-HRRST and its coupling with the DELICIOUS III double imaging ($i^2$PEPICO) spectrometer of the DESIRS beamline at the SOLEIL synchrotron facility has been described in detail in [9]. The driven section of the ICARE-HRRST has a bore of 8 mm and its length can be adjusted based on the specific needs by adding modular elements. The final part of the driven section, of 12 mm internal diameter, enters the driver section which consists of a high-pressure chamber and a fast acting, high-pressure, solenoid actuated valve. The total length of the shock tube once installed at SOLEIL is around 1.4 m. Pressure transducers (CHIMIE METAL A25L05B, 2 mm diameter) are located on the valves and spacer sections with distance 60.0 mm from each other. The final pressure transducer is 20.0 mm from the end wall. The pressure signals are acquired with a GAGE-Applied Octopus 14-bit PCIE card and used to measure the shock velocity extrapolated at the end-wall. $P_4$ is monitored by a Honeywell LM-BP211DL sensor, $P_1$ by an MKS 722B capacitance manometer, $T_1$ by K-type thermocouples close to the end-wall. This information together with the initial mixture composition are used to calculate $P_5$ and $T_5$ by solving the continuity equations. A 400 μm nozzle is installed at the end-wall and aligned to the first skimmer (1 mm orifice) of the SAPHIRS chamber. A second skimmer (2 mm orifice) is located at the entrance of the spectrometer chamber forming the second stage of the differential pumping system.

DELICIOUS III consists of a velocity map imaging (VMI) spectrometer and a modified Wiley–McLaren time-of-flight (TOF) imaging spectrometer that simultaneously detects electrons and ions, respectively. The 3D ion momentum distribution is obtained from the ion TOF referenced to the arrival time of the corresponding electron and its location on the position-sensitive detector. A second position-sensitive detector is used to collect electron images on the VMI. These images can be treated with an Abel inversion algorithm to obtain photoelectron spectra. The synchronization between DELICIOUS-III and the shock tube is performed with a NIM signal from a Stanford DG535 delay pulse generator that is sent to the Time to Digital Converter managing the data acquisition of the DELICIOUS III spectrometer. The NIM signal provides the reference time for the arrival of the photoelectrons at the position sensitive detector, while the ion TOF is measured with respect to the electron arrival, carrying the m/z kinetic information. For each shock tube experiment, the MS data are acquired for 8 ms time span covering the pre-shock and the post-shock conditions. The experiments presented in this work were obtained at a repetition rate of 1 Hz, while the photon energy chosen to ionize the fuel molecules and the products is fixed at 10 eV for toluene, 14.5 eV for carbon dioxide.

## 3 Formulation of the external calibration method

In general, the mass spectrometer signal for species *x* can be written as follows:

$$S_x = \sigma_x \cdot [x] \cdot n_{exp} \cdot D_x \cdot \eta_{set} \cdot f(P,t) \qquad (1)$$

where $\sigma_x$ is the photoionization cross section at the specific photon energy, [*x*] the concentration of species *x*, $n_{exp}$ the number of experiments, $D_x$ the discrimination factor, $\eta_{set}$ the coefficient which takes into account the efficiency of the system for the specific experimental set (function of the beamline intensity, the nozzle and skimmer sizes and relative distances etc), and *f(P,t)* the correction term as function of the pressure inside the mass spectrometer chamber and the time. For the specific case of the $CO_2$ external standard, this equation becomes

$$S_{CO_2} = \sigma_{CO_2} \cdot [CO_2] \cdot n_{CO_2\_set} \cdot D_{CO_2} \cdot \eta_{CO_2\_set} \cdot f(P,t) \qquad (2)$$

from which we can derive the expression for *f(P,t)*

$$f(P,t) = \frac{S_{CO_2}}{\sigma_{CO_2} \cdot [CO_2] \cdot n_{CO_2\_set} \cdot D_{CO_2} \cdot \eta_{CO_2\_set}} \qquad (3)$$

Substituting equation 3 into equation 1, the concentration of any species x can be derived from

$$[x] = [CO_2] \cdot \frac{S_x}{S_{CO_2}} \cdot \frac{\sigma_{CO_2}}{\sigma_x} \cdot \frac{n_{CO_2\_set}}{n_{set}} \cdot \frac{D_{CO_2}}{D_x} \cdot \frac{\eta_{CO_2\_set}}{\eta_{set}} \qquad (4)$$

The concentration of the external standard and the number of experiments are known, the ratio between signals can be obtained from the experimental measurements, while the discrimination factors can be estimated based on previous investigations. Thus, if the photoionization cross sections are measured or calculated, the only unknown in the equation is the ratio between the efficiency factors. This ratio is the same for all the species measured in a specific dataset, including the fuel molecule. Thus, its value can be derived from the following equation

$$\frac{\eta_{CO_2\_set}}{\eta_{set}} = \frac{[fuel]_0}{[CO_2]_0} \cdot \frac{S_{CO_2,t=0}}{S_{fuel,t=0}} \cdot \frac{\sigma_{fuel}}{\sigma_{CO_2}} \cdot \frac{n_{set}}{n_{CO_2\_set}} \cdot \frac{D_{fuel}}{D_{CO_2}} \qquad (5)$$

where $[fuel]_0$ and $[CO_2]_0$ are the known concentrations of fuel and external standard at time zero after the passage of the reflected shock wave.

## 4 Results

The mass spectrometer signal is proportional to the gas density (or pressure) inside the mass spectrometer chamber, which varies during the miniature shock tube cycle. The arrival of the incident shock wave at the end-wall generates a nearly instantaneous (few microseconds) rise of the thermodynamic conditions to $P_5$ and $T_5$ which results in an increment of the gas density in the molecular beam. Figure 1 shows an example of time history profile obtained averaging around 1000 experiments of toluene pyrolysis (0.1% in argon bath gas). For these pressure measurements, the nozzle is replaced by a PCB pressure transducer (113B24) covered by a thin layer of RTV. In addition to the pressure time-history, Figure 2 contains the kinetic (signal intensity/time) profiles measured with the i$^2$PEPICO spectrometer for m/z = 92 (fuel molecule) and m/z = 78 (one of the main peak products, mainly benzene) before correction, for the dataset on toluene pyrolysis. As a consequence of the transition from $P_1$ to $P_5$, the pressure in the mass spectrometer chamber builds up but at a slower rate compared to the pressure inside the HRRST. The signal for the fuel molecule increases with the arrival of the shock wave and then it stays nearly constant for around 400 μs, before dropping to nearly its baseline within 200 μs. As the fuel signal falls, products start to appear, for example m/z =78 in Figure 1. The non-idealities inside the ICARE-HRRST are larger than those in conventional shock tubes, and the variations in the pressure time-histories reflects in changes of the temperature, species concentrations and molecular beam gas density, thus affecting the signal levels. The external calibration provides a correction as a function of time for these non-ideal behaviors, allowing extraction of kinetic information in units of mole fractions.

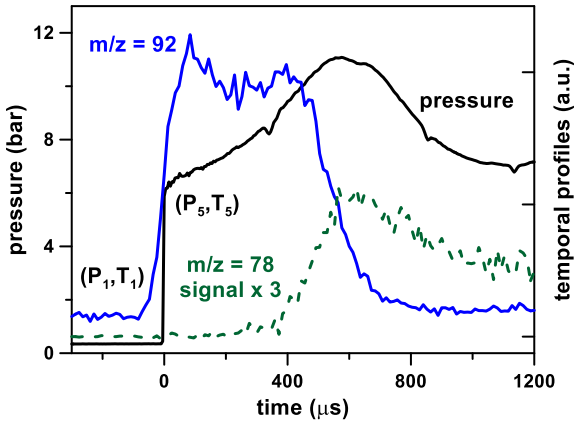


Figure 1. Toluene pyrolysis, 0.1% in argon. Pressure profile from 1000 experiments; temporal species profiles from 107 000 experiments at T = 1362±22 K and P = 6.6±0.2 bar, photon energy 10.0 eV.

The ICARE-HRRST/i²PEPICO technique was employed to perform experiments with an initial CO2 mole fraction of 0.1% in argon, presented in Figure 2 together with the m/z = 92 from the experiments in Figure 1. Carbon dioxide does not react at the thermodynamic conditions of the experiments, thus its mole fraction behind the reflected shock wave is constant. On the other hand, its signal varies due to the pressure variations inside the shock tube. The initial rise in the $CO_2$ profile is slightly faster than the case of toluene. This is probably an artifact of the large difference in the number of experiments (~ 6 000 vs 107 000) and the signal levels. Note that the $CO_2$ values have been multiplied by a factor of 3 in Figure 2. The carbon dioxide profile seems to follow a similar trend as the pressure profile in Figure 2, with an increase of the signal due to the effects of the non-idealities and the subsequent decrease due to the arrival of the rarefaction waves above 600 μs.

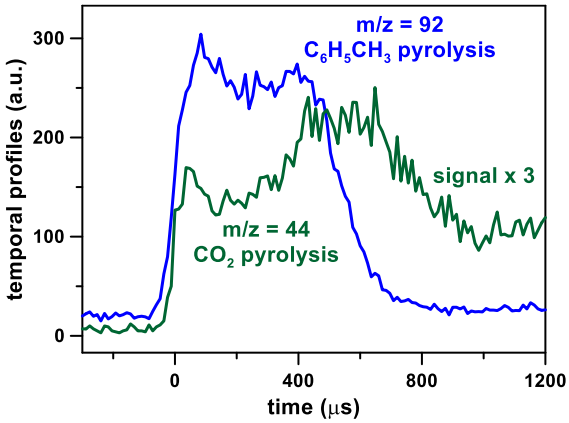


Figure 2. Temporal species profiles, m/z = 92 from toluene pyrolysis (0.1% in argon), average over 107 000 experiments at T = 1362±22 K and P = 6.6±0.2 bar, photon energy = 10.0 eV; m/z = 44 from carbon dioxide pyrolysis (0.1% in argon), average over 6 000 experiments at T = 1376±12 K and P = 6.6±0.1 bar, photon energy = 14.5 eV.

The results of the analyses obtained implementing the external standard calibration technique on the toluene pyrolysis data are presented in Figure 3. One of the main uncertainties in the development of the external calibration technique is related to the alignment between the fuel and the CO2 profiles, as the initial rise times of these two profiles are slightly different (Figure 2). In fact, in case of erroneous alignment, the noise of the original signal might be amplified by the data treatment, resulting in relatively large uncertainties. Figure 3a contains the m/z = 92 and 78 profiles from the toluene pyrolysis with the $CO_2$ profiles shifted to match i) the times of the 50% signal rises as in Figure 1 (dark dashed lines), ii) the times of the two main peaks (solid lines, $CO_2$ profile shifted by +36 μs), iii) the times at which the two profiles start rising (light dashed lines, $CO_2$ profile shifted by -24 μs). Concerning the fuel profile, the first 200 μs are affected by the different treatments, with less oscillations for the second case. This is reasonable as in the other two cases the raw m/z = 92 signal is still increasing when the $CO_2$ profile starts its descent, thus the correction factor does not match the actual m/z = 92 profile. For the three analyses, the noise in the treated signal before time zero is quite large, thus the derived information is not useful. Concerning the products, these are not significantly affected by the choice of the alignment procedure, as shown for m/z = 78, since their appearance occurs at late times. Finally, method ii) was preferred for the reduced noise.

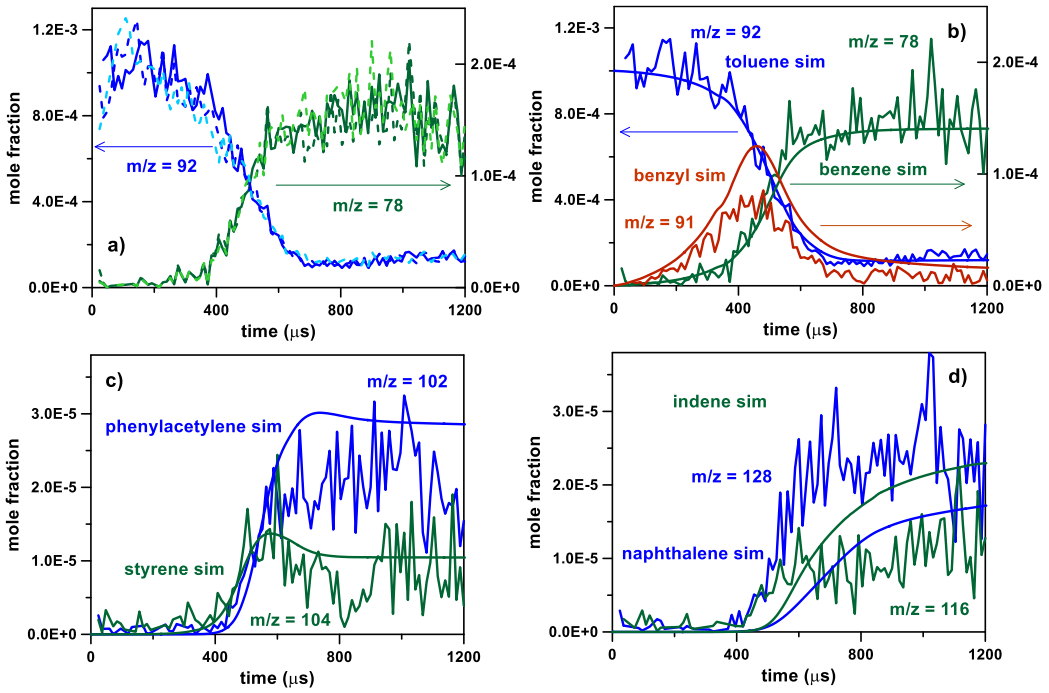


Figure 3. Temporal species profiles from toluene pyrolysis (0.1% in argon), average over 107 000 experiments at T = 1362±22 K and P = 6.6±0.2 bar, photon energy = 10.0 eV. In a), different matching between fuel and $CO_2$ profiles: solid line at the peak, light dashed line at start of the rise, dark dashed line at 50% rise. Lines in b)-c)-d) represent kinetic modeling with ICARE PAH chemistry model [14].

Figure 3b, c, and d present the temporal species profiles for the fuel and some of the main products after correction. In particular, the species were chosen if their identification could be easily obtained by comparing their photoelectron spectra with the literature ones (excluding minor contributions from isomers) and for which the cross sections have been measured and/or estimated. In particular, the absolute ionization cross sections at 10 eV for toluene, phenylacetylene, styrene, indene, and ethylbenzene were taken from the work of Zhou et al. [11], the one for benzene from Rennie et al. [12], while for naphthalene an estimated value as in [13]. Concerning carbon dioxide, its cross section at 14.5 eV was taken from the work of Hitchcock et al. [14]. In Figure 3, the solid lines represent simulations obtained with the ICARE chemical kinetic model for PAH formation and growth [15], which was validated against species profiles vs temperature from single-pulse shock tube experiments. The simulations were performed with ANSYS CHEMKIN-Pro 2021 software, batch reactor with variable pressure following the profile in Figure 1. There is an overall excellent agreement between experiments and simulations for the decomposition of the fuel and the formation of the main single-ring aromatic products, including benzene (m/z = 78), styrene (m/z = 104), and phenylacetylene (m/z = 102), especially considering that the model was not modified to match the experimental data. A peak at m/z = 91, corresponding to the benzyl radical, was also detected and measured. For this, the same parameters as for m/z = 92 were used as first approximation. The shape of the m/z = 91 profile is correctly captured by the model, as well as its concentration (considering the related uncertainties). Species profiles for larger PAH products as indene (m/z = 116) and naphthalene (m/z = 128) are shown in Figure 3d. Although the rise in the simulation profiles are delayed compared to the experiments and the absolute concentrations are not perfectly reproduced (especially in relative terms), the results are quite satisfactory considering the complexity of the chemistry involved in the PAH formation and the experimental uncertainties.

## Acknowledgment

This project has received funding from the European Research Council (ERC) under the European Union's Horizon 2020 research and innovation programme (grant agreement n° 756785).

## References

[1] W. Tsang, A. Lifshitz, Single Pulse Shock Tube, Handbook of Shock Waves, Part III: Chemical Reactions in Shock Waves, Academic Press, New York, 2001.

[2] R. S. Tranter, K. Brezinsky, D. Fulle, Design of a high-pressure single pulse shock tube for chemical kinetic investigations, Rev. Sci. Instrum., 2001, 72, 3046.

[3] A. Comandini, T. Malewicki, K. Brezinsky. Online and offline experimental techniques for polycyclic aromatic hydrocarbons recovery and measurement, Rev. Sci. Instrum., 2012, 83, 034101.

[4] R. S. Tranter, B. R. Giri, J. H. Kiefer, Shock Tube/Time-Of-Flight Mass Spectrometer for High Temperature Kinetic Studies, Rev. Sci. Instrum., 2007, 78, 034101.

[5] S. H. Dürrstein, M. Aghsaee, L. Jerig, M. Fikri, C. Schulz A shock tube with a high-repetition-rate time-of-flight mass spectrometer for investigations of complex reaction systems, Rev. Sci. Instrum., 2011, 82, 084103.

[6] R. K. Hanson, D. F. Davidson, Recent advances in laser absorption and shock tube methods for studies of combustion chemistry, Prog. Energy Combust. Sci., 2014, 44, 103–114.

[7] R. S. Tranter, P. T. Lynch, A miniature high repetition rate shock tube, Rev. Sci. Instrum., 2013, 84, 094102.

[8] P. T. Lynch, T. P. Troy, M. Ahmed, R. S. Tranter, Probing Combustion Chemistry in a Miniature Shock Tube with Synchrotron VUV Photo Ionization Mass Spectrometry, Anal. Chem., 2015, 87, 2345–2352.

[9] S. Nagaraju, R. S. Tranter, F. E. Cano Ardila, S. Abid, P. T. Lynch, G. A. Garcia, J. F. Gil, L. Nahon, N. Chaumeix, A. Comandini, Pyrolysis of ethanol studied in a new high-repetition-rate shock tube coupled to synchrotron-based double imaging photoelectron/photoion coincidence spectroscopy, Comb. Flame, 2021, 226, 53–68.

[10] L. Nahon, N. de Oliveira, G. A. Garcia, J.F. Gil, D. Joyeux, B. Lagarde, F. Polack, DESIRS : a state-of-the-art VUV beamline featuring high resolution and variable polarization for spectroscopy and dichroism at SOLEIL, J. Phys.: Conf. Ser., 2012, 425, 122004.

[11] Z. Zhou, M. Xie, Z. Wang, F. Qi, Determination of absolute photoionization cross-sections of aromatics and aromatic derivatives, Rapid Commun. Mass Spectrom. 2009, 23, 3994–4002.

[12] E. E. Rennie, C. A. F. Johnson, J. E. Parker, D. M. P. Holland, D. A. Shaw, M. A. Hayes, A photoabsorption, photodissociation and photoelectron spectroscopy study of C6H6 and C6D6, Chem. Phys. 1998, 229, 107–123.

[13] Edited by JiuZhong Yang and Combustion Team. Photonionization Cross Section Database (Version 2.0). National Synchrotron Radiation Laboratory, Hefei, China. (2017).

[14] A. P. Hitchcock, C. E. Brion, M. J. Van der Wiel, Absolute Oscillator Strengths for Valence-Shell Ionic Photofragmentation of N2O and CO2 (8–75 eV), Chem Phys, 1980, 45, 461–478.

[15] W. Sun, A. Hamadi, S. Abid, N. Chaumeix, A. Comandini, Detailed experimental and kinetic modeling study of toluene/C2 pyrolysis in a single-pulse shock tube, Combust. Flame, 2021, 226, 129–142.